

Nuclear tetrahedral configurations at spin zero

Krzysztof Zborecki¹, Paul-Henri Heenen² and Piotr Magierski¹

¹*Faculty of Physics, Warsaw University of Technology,
ul. Koszykowa 75, 00-662 Warsaw, Poland and*

²*Service de Physique Nucléaire Théorique, U.L.B - C.P. 229, B 1050 Brussels, Belgium*

(Dated: November 11, 2018)

The possibility of the existence of stable tetrahedral deformations at spin zero is investigated using the Skyrme-HFBCS approach and the generator coordinate method (GCM). The study is limited to nuclei in which the tetrahedral mode has been predicted to be favored on the basis of non self-consistent models. Our results indicate that a clear identification of tetrahedral deformations is unlikely as they are strongly mixed with the axial octupole mode. However, the excitation energies related to the tetrahedral mode are systematically lower than those of the axial octupole mode in all the nuclei included in this study.

PACS numbers: 21.60.Jz, 21.10.Re, 27.60.+j, 27.50.+e, 27.70.+q

I. INTRODUCTION

Exotic shapes of the nuclear density have always attracted the interest of physicists. In this respect, the octupole degree of freedom has played a special role. Axial octupole deformations are well established, both experimentally and theoretically [1], in several regions of the nuclear chart. It has also been shown that non axial octupole shapes are competitive with the axial ones in specific nuclei [2]. However, octupole deformations are more subtle than quadrupole ones. Stable static octupole deformations correspond usually to shallow minima as a function of the octupole deformation [3, 4, 5]. Dynamical studies have shown that octupole correlations in the ground state manifest themselves predominantly by a spreading of the wave function around the left-right symmetric mean-field configuration [6].

Nuclear tetrahedral deformations have been recently investigated in Refs.[7, 8, 9]. Symmetry arguments show that tetrahedral deformations induce a 4-fold degeneracy of the single-particle spectra. Based on this peculiar shell structure, the stability of such configurations has been conjectured in specific nuclei. Such a large degeneracy results indeed in large gaps in the single-particle spectrum and increases the shell effects for specific values of the neutron and proton numbers. Those values have been dubbed 'tetrahedral magic numbers' and have been determined using a microscopic-macroscopic model based on a Woods-Saxon potential[7, 8, 9, 10, 11, 12].

However these conjectures almost exclusively originate from approaches based on non self-consistent average nuclear potentials, with only a limited support of self-consistent calculations. It is therefore clearly necessary to test their validity in the framework of up-to-date theories using modern energy density functionals. We address this issue in the present paper in the framework of self-consistent mean-field methods using Skyrme interactions. Since to go beyond a pure mean-field approach has been shown to be crucial for octupole deformations, we have also studied the stability of tetrahedral shapes using the generator coordinate method (GCM). This study

is focused on nuclei in which the tetrahedral mode has been predicted to be favored: ^{80,98,110}Zr, ^{152–156}Gd and ¹⁶⁰Yb. It extends our previous study which was limited to ^{80,98}Zr[13, 14] (Ref. I) by considering the dynamical coupling between the axial octupole and the tetrahedral degrees of freedom. Since tetrahedral shapes are generated by the non-axial intrinsic octupole moment $Q_{32} \propto r^3(Y_{32} + Y_{3-2})$ it is likely that they are in strong competition with axial octupole shapes. Most details about our method can be found in Ref. I, those on the GCM in Ref. [15] and on its application to 2-dimensional octupole calculations in Ref. [17].

Our aim in this study is to determine whether there are situations in which a configuration can be unambiguously identified as tetrahedral. We will therefore first identify which are the possible coexisting structures in the nuclei for which tetrahedral deformations have been predicted. We will then study whether some of these configurations provide clear signatures of tetrahedral shapes.

II. MEAN-FIELD CALCULATIONS AND PARITY PROJECTION

Octupole deformations of the nuclear density are generated by introducing in the HFBCS equations the axial $Q_{30} \propto r^3 Y_{30}$ and the triaxial $Q_{32} \propto r^3(Y_{32} + Y_{3-2})$ moments as constraining operators. This last one is the operator generating tetrahedral deformations. The details of the HFBCS calculations have been described in Ref. I. The pairing interaction strength has been adjusted to reproduce 'experimental pairing gaps' in the same way as described in Ref. I. In particular the standard prescription based on the odd-even difference of binding energies has been used [18]. The pairing strength for ⁹⁸Zr and ¹¹⁰Zr has been adjusted to reproduce the pairing gap in ¹⁰²Zr. In Gd isotopes the pairing strength has been adjusted to reproduce pairing gaps in ¹⁵⁴Gd. For studies of ⁸⁰Zr and ¹⁶⁰Yb the pairing strength has been adjusted for each of these nuclei individually. These reference nuclei have been chosen in order to minimize the influence of

deformation changes for the determination of the pairing gap.

The experimental data suggest that all the nuclei in which tetrahedral deformations have been predicted theoretically have a well deformed ground state (with the possible exception of ^{98}Zr). A first question to address is whether a spherical configuration may coexist at low excitation energy in any of the studied nuclei. As we shall see in the following, the single-particle pattern typical of a tetrahedral configuration is very well preserved close to sphericity. Therefore a 'tetrahedral magic' nucleus in which the spherical configuration is at low energy represents a particularly promising case of the existence of tetrahedral configurations. Let us first focus on the case of ^{110}Zr for which the variation of the energy as a function of the axial quadrupole deformation is shown in Fig. 1. Octupole deformations are set to zero for all values of the quadrupole moment. The calculations have been performed for three representative Skyrme parameterizations. A deformed prolate ground state at large deformation is obtained for all three interactions. It coexists with an oblate minimum and, in the case of SLy4 and SkM*, with a local minimum for the spherical configuration. It is only for the SLy4 parameterization that the spherical and the prolate minima are almost degenerate.

The case of ^{110}Zr illustrates well the energy dependence on the quadrupole degree of freedom obtained for all studied nuclei with the three Skyrme forces. The ground state corresponds in all cases to a deformed prolate minimum (with the only exception of ^{80}Zr for the SLy4 parameterization but this is in clear contradiction with the experimental data [16]). The spherical configurations are excited by a few MeV, except in some Zr isotopes where depending on the Skyrme parameterization they are obtained at excitation energies smaller than 1 MeV.

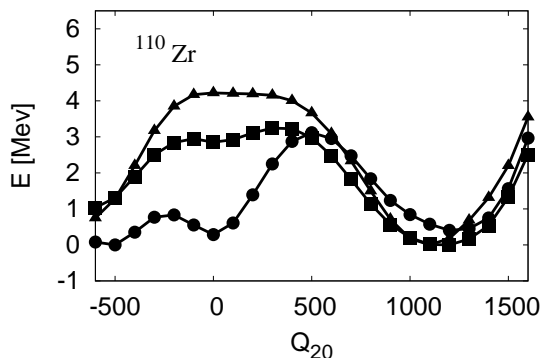


FIG. 1: Variation of the total mean-field energy as a function of the quadrupole Q_{20} moment (in fm^2). Triangles, squares and circles denote results obtained using the SIII, SkM* and SLy4 parameterizations of the Skyrme force, respectively

A first question that must be answered is how this picture is affected by tetrahedral deformations and whether the magnitude of the energy gain obtained around the spherical minimum is large enough to bring its energy

close to that of the deformed ground state.

The variation of the mean-field energy with octupole deformations when the quadrupole moment is constrained to be zero is shown in Fig. 2 for the six nuclei that we have selected. These results have been obtained with the SLy4 Skyrme parameterization and their dependence on the choice of the parameterization is illustrated by results obtained for ^{110}Zr with SIII. Note that, contrary to Fig. 1, the HFBCS results are very similar for both interactions. We have also checked for several nuclei and for SkM* that the behaviour of the HFBCS energy as a function of the octupole degrees of freedom is qualitatively similar in all cases.

The octupole deformations are parameterized by dimensionless parameters proportional to the octupole moments (see Ref. I). There is no direct connection between the values of β_{30} and β_{32} and one must be cautious when comparing axial and tetrahedral deformation energy curves. The only nucleus for which a sizeable tetrahedral minimum is obtained is ^{156}Gd with an energy gain of 500 keV with respect to the spherical configuration. The energy is rather flat as a function of both β_{30} and β_{32} for the other nuclei, although the meaning of this shallowness can only be made precise by dynamical calculations. The energy curve obtained for ^{110}Zr with SIII is only marginally different from that of SLy4, with a tetrahedral minimum 100 keV below the spherical point.

These mean-field calculations have been performed using a single constraint on either the Q_{30} or Q_{32} moments. Since the unconstrained degrees of freedom are completely relaxed (except for the quadrupole moment and either Q_{30} or Q_{32} which were set to zero) by the variational procedure, there is no guarantee that the unconstrained moments remain equal to zero (except those that are forbidden due to the imposed symmetry conditions - see Ref. I) for all values of the constraint. Nevertheless, the behavior typical of the tetrahedral symmetry is largely preserved up to a deformation of $\beta_{32} \approx 0.2-0.3$. Up to these values, the single-particle states exhibit the 4-fold degeneracies characteristic for the point group T_d^D . In general, the single particle energies as a function of Q_{32} exhibit more bunching as compared to the Q_{30} direction. However, this does not translate into a lower energy for the tetrahedral configuration.

As a typical example, the variation of the single-particle energies as a function of octupole deformations is shown in Fig. 3 for ^{110}Zr . One can see that the single particle states are still almost degenerate at β_{32} equal to 0.15 but not at β_{30} equal to 0.15, which is in both cases the deformation beyond which the mean-field energy starts to increase. Note also that both the tetrahedral and the spherical configurations have a similar single-particle structure since there are no level crossings between these configurations. The same is true for the axial octupole configuration. Moreover the HFBCS calculations indicate almost no barrier between tetrahedral and axial octupole minima. These facts indicate that all the three configurations may be strongly mixed when

the octupole collective dynamics is taken into account (see next section).

Since tetrahedral deformations break parity, projection on parity gives rise to an energy gain for the positive parity as soon as the octupole moments have a non zero value and it generates a distinct energy curve for the negative parity. We have restored both particle number and parity by projecting the mean-field wave functions. The projected potential energy is defined as:

$$E(N, Z, \beta_{3\mu})_{\pm} = \frac{\langle \phi(\beta_{3\mu}) | \hat{H} \hat{P}_{(\pm, N, Z)} | \phi(\beta_{3\mu}) \rangle}{\langle \phi(\beta_{3\mu}) | \hat{P}_{(\pm, N, Z)} | \phi(\beta_{3\mu}) \rangle}, \quad (1)$$

where $|\phi(\beta_{3\mu})\rangle$ are HFBCS wave functions generated with the constraint $\langle \phi(\beta_{3\mu}) | \hat{Q}_{3\mu} | \phi(\beta_{3\mu}) \rangle = C_{\mu} \beta_{3\mu}$, where $C_0 = \frac{3}{4\pi} A^2 r_0^3$, $C_2 = C_0 / \sqrt{2}$ with $A = N + Z$ and $r_0 = 1.2 fm$ (see Ref. I). The operator $\hat{P}_{(\pm, N, Z)}$ is the product of operators projecting on $\pi = \pm 1$ parity and on N neutrons and Z protons. The parity-projected energies are shown in Fig. 4, except for ^{80}Zr and ^{98}Zr which were already discussed in Ref. I.

The situation is similar to that discussed already in Ref.[13, 14]. The positive parity curves exhibit a small minimum for nonzero values of β_{30} and β_{32} . The energy gain due to the parity restoration is of the order of 1 MeV for both axial octupole and tetrahedral deformations (see Fig.4). In fact for all nuclei considered (with the exception of ^{160}Yb) the axial octupole minimum has a slightly lower energy than the tetrahedral one (see table I).

The dependence of energy on octupole deformations is not significantly modified by the projection on positive parity. An interesting property of the particle projection is that it makes the results rather weakly dependent on the pairing strength, in contrast to pure mean-field calculations. We have checked that the differences between the energy of the octupole minima and that of the spherical configuration are not significantly modified by a variation of the pairing strength within the interval between half and twice the physical value. This holds for both the positive and negative parity states. The main effect of an increase of the pairing strength is an increase of the energy difference between the positive and negative parity minima.

III. TWO-DIMENSIONAL GCM

To be unambiguously identified experimentally, tetrahedral deformations should have a clear signature, which allows to distinguish them from axial octupole deformations. The GCM enables to study the coupling between both octupole modes and to see whether tetrahedral shapes can be separated from axial octupole shapes. We have therefore performed two-dimensional GCM calculations in which the axial and non axial octupole shapes are coupled. This coupling was not considered in Ref. I, where separate dynamical calculations were performed

along the collective paths determined by non zero Q_{30} and Q_{32} values, respectively. The method we apply is similar to that introduced by Skalski et al. [17].

A collective wave function is constructed by mixing the mean-field states corresponding to different values of the octupole moments, after their projection on particle numbers:

$$|\Psi\rangle = \int f(\beta_{30}, \beta_{32}) \hat{P}_{(N, Z)} |\phi(\beta_{30}, \beta_{32})\rangle d\beta_{30} d\beta_{32} \quad (2)$$

The coefficients $f(\beta_{30}, \beta_{32})$ are determined by minimizing the total energy of the collective wave function $|\Psi\rangle$.

Our collective space forms a plane specified by Q_{30} and Q_{32} , or equivalently by β_{30}, β_{32} . This requires to consider HFBCS states inside a rectangle specified by "corners": $(\pm\beta_{30max}, \pm\beta_{32max})$. However the full problem can be decomposed in four subspaces by introducing combinations of states in the four quadrants. Starting from $|\phi_1\rangle = |\phi(\beta_{30}, \beta_{32})\rangle$, one constructs the four states:

$$\begin{aligned} |\phi_2\rangle &= |\phi(-\beta_{30}, -\beta_{32})\rangle = \hat{P}|\phi_1\rangle, \\ |\phi_3\rangle &= |\phi(-\beta_{30}, +\beta_{32})\rangle = \hat{P}_{xy}\hat{P}|\phi_1\rangle, \\ |\phi_4\rangle &= |\phi(+\beta_{30}, -\beta_{32})\rangle = \hat{P}_{xy}|\phi_1\rangle, \end{aligned}$$

where \hat{P} is the parity operator and \hat{P}_{xy} is the reflection operation in which x and y coordinates are exchanged. Thus, one needs to generate only the HFBCS basis in 1/4 of the rectangle and extends it to the full square thanks to these relations. Another interest of this decomposition is that \hat{P} and \hat{P}_{xy} commute with the Hamiltonian. This means that they can be used to label GCM eigenstates. Both \hat{P} and \hat{P}_{xy} are projectors, so the quantum numbers associated to each operator take the values ± 1 . From the wave functions $|\phi_i\rangle$, $i = 1, 2, 3, 4$, one can define a new basis in which both \hat{P} and \hat{P}_{xy} are diagonal, namely:

$$\begin{aligned} |\Phi_{++}\rangle &= \frac{1}{2}(|\phi_1\rangle + |\phi_2\rangle + |\phi_3\rangle + |\phi_4\rangle), \\ |\Phi_{--}\rangle &= \frac{1}{2}(|\phi_1\rangle - |\phi_2\rangle + |\phi_3\rangle - |\phi_4\rangle), \\ |\Phi_{-+}\rangle &= \frac{1}{2}(|\phi_1\rangle - |\phi_2\rangle - |\phi_3\rangle + |\phi_4\rangle), \\ |\Phi_{+-}\rangle &= \frac{1}{2}(|\phi_1\rangle + |\phi_2\rangle - |\phi_3\rangle - |\phi_4\rangle), \end{aligned}$$

where the first index of $|\Phi_{kl}\rangle$ denotes the eigenvalue with respect to parity and the second index with respect to $x - y$ reflection. One can easily check that $|\Phi_{+-}\rangle$ is identically zero in the absence of either axial or tetrahedral deformations, while $|\Phi_{-+}\rangle$ and $|\Phi_{--}\rangle$ are zero when β_{30} or β_{32} are zero, respectively. For this reason, we have dubbed the excited states corresponding to $k = l = -1$ tetrahedral excitations, those corresponding to $k = -1, l = +1$ axial excitations and those corresponding to $k = 1, l = -1$ mixed octupole excitations.

In this basis $|\Phi_{kl}\rangle$, the Hamiltonian does not couple states corresponding to different values of k and l and

the GCM equation decomposes into four equations for each set (k, l) . The resulting GCM wave functions are expressed by:

$$|\Psi_{kl}\rangle = \int f(\beta_{30}, \beta_{32}) \hat{P}_{(N,Z)} |\Phi(\beta_{30}, \beta_{32})_{kl}\rangle d\beta_{30} d\beta_{32} \quad (3)$$

We have restricted this study by imposing the quadrupole moment to be fixed. A full calculation would require to consider the octupole and quadrupole modes simultaneously, which would be a huge computational task, well beyond the scope of the present study. Our aim is indeed only to determine the most favourable scenario of coupling between axial octupole mode and the non axial Q_{32} mode generating the tetrahedral deformation.

We have first performed a calculation in the vicinity of the deformed ground state of two nuclei, ^{110}Zr and ^{154}Gd . The results are shown in Table II.

The correlation energy due to the octupole modes is defined by:

$$E_{corr} = E(N, Z, sph) - E_{++},$$

where $E(N, Z, sph)$ is the energy of the particle number projected spherical configuration and E_{++} is the lowest positive-parity energy obtained in the GCM. The value of this correlation energy is rather small for both nuclei, indicating a weak effect of octupole correlations in the ground state.

The lowest octupole excitation corresponds in both cases to the axial octupole mode. The non axial octupole excitation is only slightly larger in energy for ^{110}Zr but both modes being above 4 MeV of excitation are very unlikely to survive to the coupling to any other modes. The situation is slightly more favorable in ^{154}Gd , although in this case, the non axial excitation is nearly 1 MeV above the axial octupole one. Note that in the vicinity of a deformed ground state, one cannot identify a non axial Q_{32} mode with tetrahedral deformations, since the tetrahedral symmetry is broken by large quadrupole deformations.

In view of the very unfavorable conditions obtained when the quadrupole moment is large, we have continued this study by looking to the octupole properties around the spherical configuration. The GCM results are summarized in Table III. We have performed calculations with two sets of mean-field wave functions corresponding to 16 and 25 positive octupole deformations respectively, to check the accuracy of the results. The difference between both sets of results shows that the accuracy obtained with a 25 wave-function basis set is better than 100 keV. Note that the excellent agreement obtained by using two different basis sets is also a test that our results are not affected by the pathology that can appear when working an energy density functional[19].

The largest gain is obtained for ^{110}Zr . It is of a similar order of magnitude than the energy gain due to quadrupole correlations in deformed nuclei [20]. A full

study of the energy gain due to the coupling between different modes remain to be done but the results of Ref [20] seem to indicate that these energy gains quickly saturate in models based on self-consistent mean-field wave functions.

Dynamical deformations associated with the lowest GCM solutions corresponding to quantum numbers k and l are defined by:

$$\tilde{\beta}_{3\mu} = \sum_{\beta_{3\mu}} \beta_{3\mu} g_{kl}^2(\beta_{30}, \beta_{32}), \quad (4)$$

for $\mu = 0, 2$, where g_{kl} is the collective wave function for parity k and for an eigenvalue l associated with the operator \hat{P}_{xy} (see Ref. [15] for the relation between the collective wave function g and the GCM function f). For all nuclei that we have studied the dynamical deformations $\tilde{\beta}_{30}$ and $\tilde{\beta}_{32}$ of the lowest positive parity GCM solutions are smaller than 0.1. The ground state collective wave function is rather isotropic as a function of Q_{30} and Q_{32} . It shows a similar spreading as a function of axial and tetrahedral octupole deformations.

The first negative parity state has an excitation energy comprised between 1.0 and 2.3 MeV, the tetrahedral mode being systematically the lowest one. The largest differences $E_{+-} - E_{--}$ between both octupole modes occur for ^{110}Zr where it is around 0.8 MeV and for ^{156}Gd where it is around 0.5 MeV.

The ratio between the B(E3) values obtained for both modes are given in Table IV. Better than the absolute values of these quantities which are not well defined in an angular momentum unprojected model, these ratios are good indicators whether these states have a specific signature in their deexcitation spectrum. In the first column are given the ratios corresponding to the transitions from the tetrahedral and the axial excited states to the ground state. The second column corresponds to the ratios of the transitions between the mixed octupole states to the tetrahedral and the axial excitations. This ratio oscillates in all cases around 1 which suggests that the spectrum of GCM excitations resembles to a large extent a harmonic spectrum. The only noticeably deviation occurs in the case of ^{110}Zr where the transition from the tetrahedral state to the lowest GCM state is decreased by about 30% as compared to the deexcitation of the axial octupole vibration.

IV. CONCLUSIONS

We have investigated the possible existence of stable tetrahedral configurations in nuclei in which they were predicted on the basis of non self-consistent models. Our calculations have been based on several parametrization of the Skyrme interaction, with only marginal differences between the results. The coupling between the axial and tetrahedral octupole modes has been studied with the GCM, in the absence of quadrupole deformations. Our

results do not support the prediction that tetrahedral deformations should have a definite signature:

- The susceptibility of the spherical configuration towards tetrahedral deformations is rather weak and pairing effects wash out the shell effects. Moreover the tetrahedral minimum is accompanied by an axial octupole minimum of similar depth.
- The correlation energy associated with shape fluctuations and parity restoration lowers substantially the mean-field energy. However the dynamic octupole deformations in the ground state state is rather small. Moreover axial and non axial octupole deformations are strongly coupled.
- The excitation energies of states associated with tetrahedral shapes are systematically lower than those corresponding to the axial octupole mode. However the $B(E3)$ ratios do not distinguish between these modes.

The prospects for the experimental detection of the tetrahedral configurations at spin zero are thus rather poor. It seems that the increased shell effects due to the tetrahedral mode do not provide a sufficient condition for the existence of a stable tetrahedral deformation. At spin zero, stable tetrahedral configurations seem unlikely.

Their trace may be manifested in nuclear vibrations in negative parity bands but the $B(E3)$ values indicate that there is no way to distinguish the tetrahedral modes from the axial octupole modes by looking to the decay probabilities. It should be noted that our study does not rule out the possibility of the existence of rotating tetrahedral configurations. Several of the predicted tetrahedral nuclei are however strongly deformed in their ground state and a mixing of octupole and quadrupole deformations would make still more problematic the extraction of a tetrahedral signature.

Acknowledgments

Discussions with M. Bender, J. Dobaczewski, P. Olbratowski, W. Satuła and J. Skalski are gratefully acknowledged. This work has been supported in part by the Polish Ministry of Science under contract No. N N202 328234, the Foundation for Polish Science (FNP), the PAI P6-23 of the Belgian Office for Scientific Policy and the US Department of Energy Grant No. DE-FC02-07ER41457.

Numerical calculations were performed at the Interdisciplinary Centre for Mathematical and Computational Modelling (ICM) at Warsaw University.

-
- [1] P. Butler and W. Nazarewicz, *Rev. Mod. Phys.* **68** 349 (1996).
- [2] J. Skalski, *Phys. Lett* **B274** 1 (1992)
- [3] P. Bonche, P.-H.H. Heenen, Flocard and D. Vautherin, *Phys. Lett.* **B175** 387 (1986)
- [4] L. Egido and L. Robledo *Nucl. Phys.* **A494** 85 (1989)
- [5] J. Engel, M. Bender, J. Dobaczewski, J.H. Jesus and P. Olbratowski, *Phys. Rev.* **C68** 025501 (2003)
- [6] J. Meyer, P. Bonche, M. Weiss, H. Flocard and P.-H. Heenen, *Nucl. Phys.* **A588** 597 (1995)
- [7] X. Li and J. Dudek, *Phys. Rev.* **C49** R1250 (1994).
- [8] J. Dudek, A. Gózdź, N. Schunck, M. Miśkiewicz, *Phys. Rev. Lett.* **88** 252502 (2002); N. Schunck, J. Dudek, A. Gózdź and P.H. Regan, *Phys. Rev.* **C69** 061305(R) (2004).
- [9] J. Dudek, A. Gózdź and N. Schunck, *Acta Phys.Polon.* **B34** 2491 (2003); N. Schunck, J. Dudek, *Int.J.Mod.Phys.* **E13** 213 (2004).
- [10] N. Schunck, P. Olbratowski, J. Dudek, J. Dobaczewski, *Int.J.Mod.Phys.* **E15** 490 (2006).
- [11] J. Dudek, D. Curien, N. Dubray, J. Dobaczewski, V. Pagnon, P. Olbratowski and N. Schunck, *Phys. Rev. Lett.* **97**, 072501 (2006).
- [12] J. Dudek, J. Dobaczewski, N. Dubray, A. Gozdz, V. Pagnon, N. Schunck, *Int.J.Mod.Phys.* **E16** 516 (2007).
- [13] K. Zberecki, P. Magierski, P.-H. Heenen, N. Schunck, *Phys. Rev.* **C74** 051302(R) (2006).
- [14] K. Zberecki, P. Magierski, P.-H. Heenen, N. Schunck, *Int. J. Mod. Phys.* **E16** 533 (2007) 533.
- [15] M. Bender, P.-H. Heenen, and P.-G. Reinhard, *Rev. Mod. Phys.* **75** 121 (2003).
- [16] C. J. Lister, M. Campbell, A. A. Chishti, W. Gelletly, L. Goettig, R. Moscrop, B. J. Varley, A. N. James, T. Morrison, H. G. Price, J. Simpson, K. Connel, and O. Skeppstedt, *Phys. Rev. Lett.* **59**, 1270 (1987).
- [17] J. Skalski, P.-H. Heenen, P. Bonche, H. Flocard and J. Meyer, *Nucl. Phys.* **A551** 109 (1993).
- [18] J. Dobaczewski, P. Magierski, W. Nazarewicz, W. Satuła and Z. Szymański, *Phys. Rev.* **C63** 024308 (2001).
- [19] D. Lacroix, T. Duguet and M. Bender, arXiv:0809.2041v1
- [20] M. Bender, G. F. Bertsch, and P.-H. Heenen, *Phys. Rev. C* **73**, 034322 (2006).

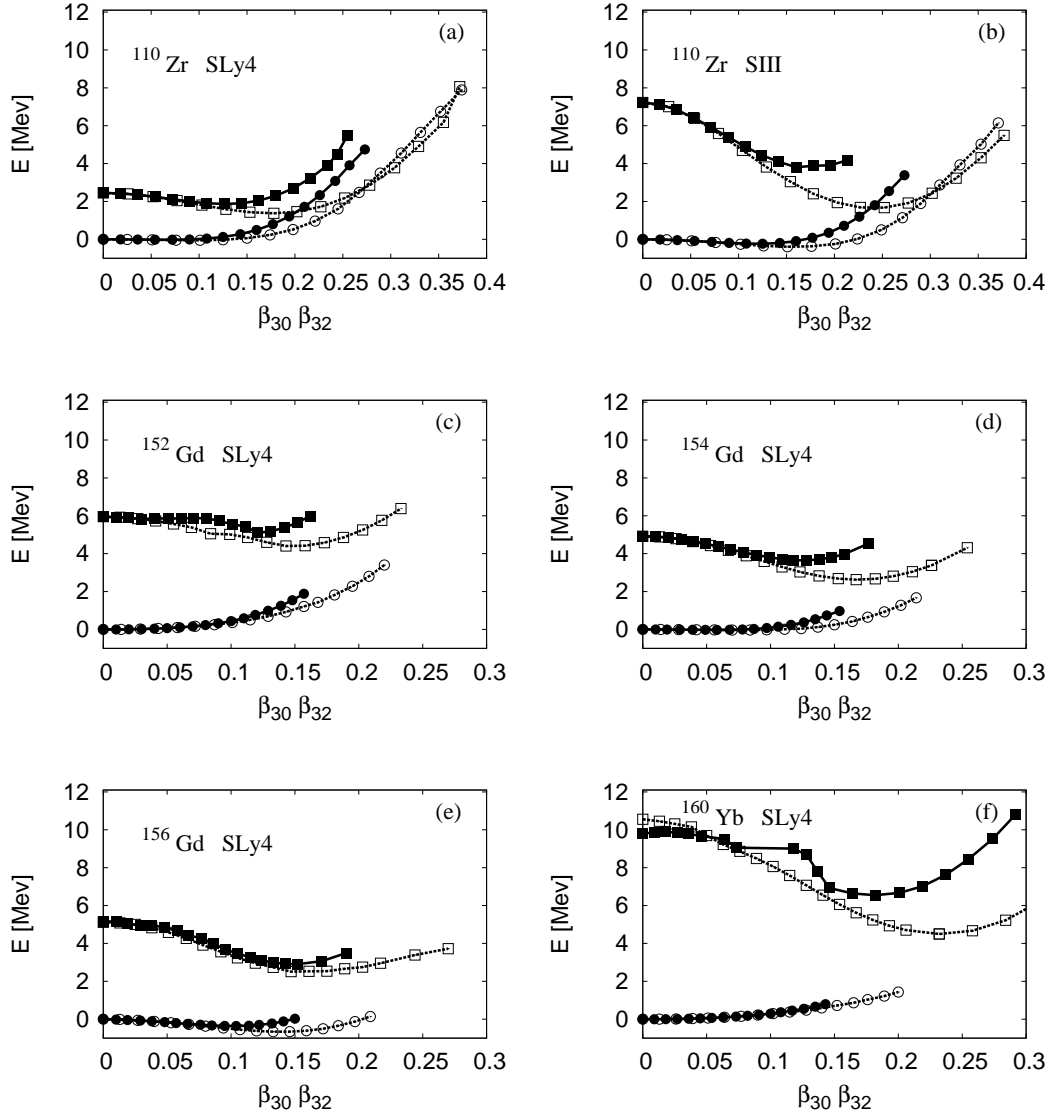


FIG. 2: Total mean-field energy obtained with the HF (squares) and HFBCS (circles) methods as a function of the dimensionless β_{30} (filled symbols) and β_{32} (open symbols) deformation parameters.

	SLy4		SIII	
	β_{30}	β_{32}	β_{30}	β_{32}
^{110}Zr	-1.25	-0.98	-1.12	-0.96
^{152}Gd	-1.09	-0.93	-	-
^{154}Gd	-1.13	-0.92	-	-
^{156}Gd	-1.16	-1.14	-	-
^{160}Yb	-1.19	-1.20	-	-

TABLE I: Energies (in MeV) of the positive parity configurations with respect to the spherical configurations for axial (β_{30}) and tetrahedral (β_{32}) configurations.

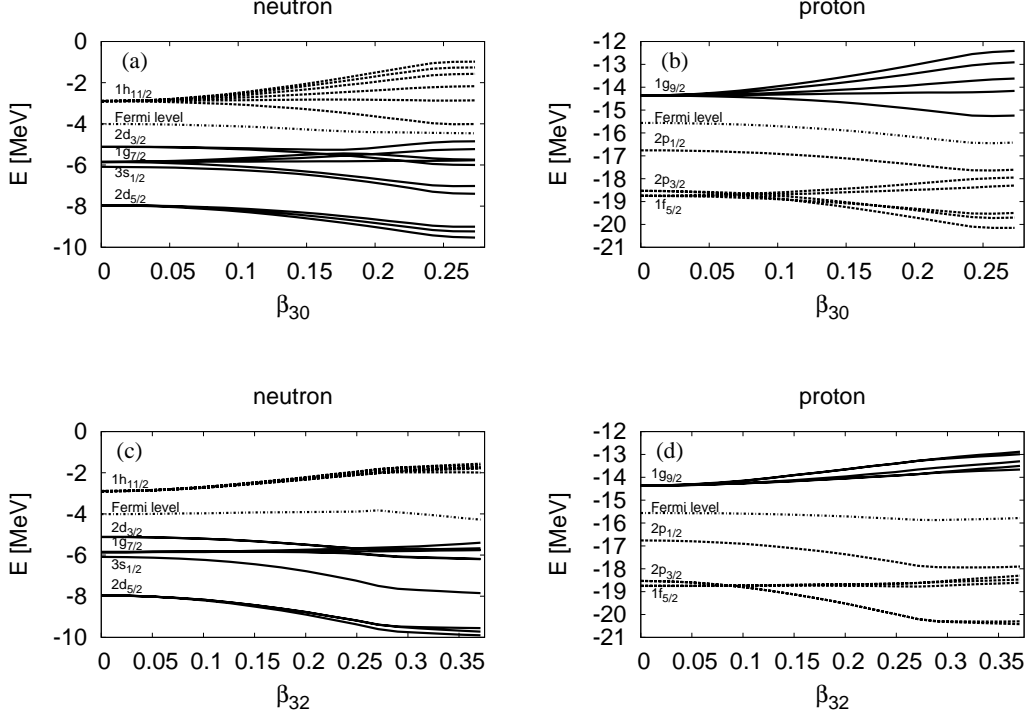


FIG. 3: Single-particle energies as a function of octupole deformation β_{30} and β_{32} for ^{110}Zr calculated for SLy4 force. The positive and negative parity levels are denoted by solid and dashed lines, respectively.

SLy4	E_{exc} (MeV)	E_{corr} (MeV)	π	π_{xy}	$\tilde{\beta}_{30}$	$\tilde{\beta}_{32}$
^{110}Zr	0	1.222	+1	+1	0.08	0.06
	4.535	-	-1	-1	0.07	0.17
	4.282	-	-1	+1	0.15	0.04
	7.423	-	+1	-1	0.19	0.24
^{154}Gd	0	2.228	+1	+1	0.05	0.06
	2.892	-	-1	-1	0.06	0.10
	1.998	-	-1	+1	0.12	0.04
	5.005	-	+1	-1	0.12	0.10

TABLE II: Excitation energies, correlation energies and dynamical deformations of the lowest four states obtained in 2-dim GCM. π and π_{xy} denote the parity and P_{xy} quantum numbers, respectively.

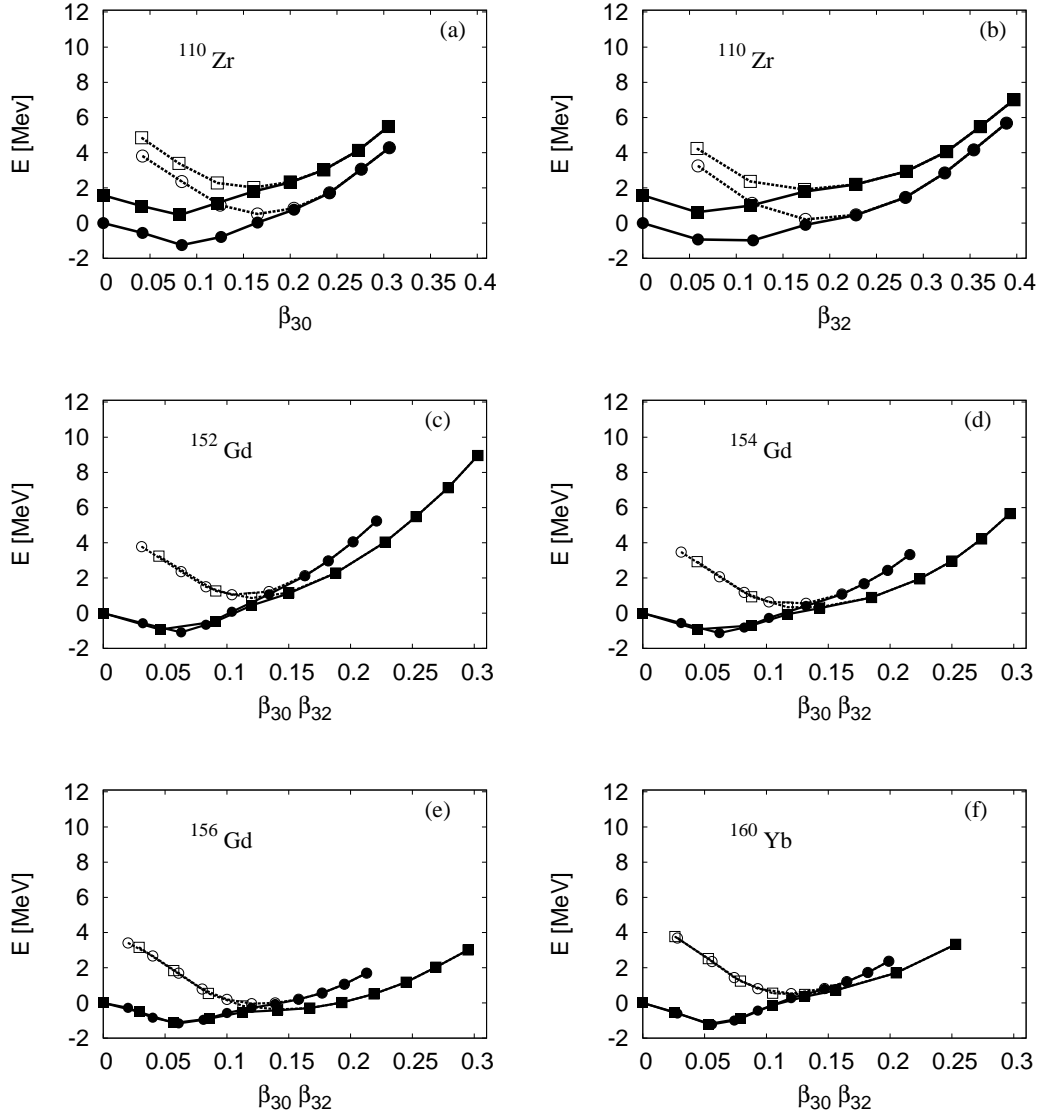


FIG. 4: Parity and particle number projected energies as a function of the octupole deformations β_{30} and β_{32} . In the two top subfigures (a and b) corresponding to ^{110}Zr , the results obtained with the SLy4 (circles) and SIII (squares) are compared. In the other subfigures, only calculations performed with SLy4 are shown. The circles and squares denote then the energies as a function of β_{30} and β_{32} , respectively. In all subfigures filled and open symbols refer to positive and negative parity, respectively.

SIII	E_{exc} (MeV)	E_{corr} (MeV)	$\Delta_{16/25}$	π	π_{xy}	$\tilde{\beta}_{30}$	$\tilde{\beta}_{32}$	$2E_{qp}^p$ (MeV)	$2E_{qp}^n$ (MeV)
^{80}Zr	0	2.116	0.15	+1	+1	0.07	0.06	2.786	3.518
	2.832	-	0.06	-1	-1	0.05	0.18		
	2.854	-	0.01	-1	+1	0.14	0.00		
	8.275	-	0.16	+1	-1	0.13	0.17		
^{98}Zr	0.0	1.184	0.02	+1	+1	0.07	0.04	2.114	2.66
	2.128	-	0.12	-1	-1	0.04	0.25		
	1.732	-	0.09	-1	+1	0.19	0.02		
	6.628	-	0.12	+1	-1	0.17	0.23		
SLy4	E_{exc} (MeV)	E_{corr} (MeV)	$\Delta_{16/25}$	π	π_{xy}	$\tilde{\beta}_{30}$	$\tilde{\beta}_{32}$	$2E_{qp}^p$ (MeV)	$2E_{qp}^n$ (MeV)
^{98}Zr	0	2.660	0.07	+1	+1	0.10	0.08	1.96	1.78
	2.393	-	0.06	-1	-1	0.08	0.21		
	2.639	-	0.05	-1	+1	0.18	0.06		
	6.127	-	0.02	+1	-1	0.17	0.17		
^{110}Zr	0	3.303	0.01	+1	+1	0.09	0.10	1.612	2.72
	1.764	-	0.01	-1	-1	0.06	0.22		
	2.188	-	0.01	-1	+1	0.17	0.06		
	4.936	-	0.01	+1	-1	0.16	0.20		
^{152}Gd	0	2.791	0.00	+1	+1	0.05	0.06	2.884	2.78
	2.018	-	0.00	-1	-1	0.04	0.13		
	2.233	-	0.00	-1	+1	0.11	0.05		
	4.922	-	0.01	+1	-1	0.12	0.12		
^{154}Gd	0	3.054	0.00	+1	+1	0.06	0.07	2.566	3.0
	1.507	-	0.01	-1	-1	0.05	0.14		
	1.857	-	0.01	-1	+1	0.12	0.05		
	4.134	-	0.00	+1	-1	0.11	0.02		
^{156}Gd	0	3.085	0.10	+1	+1	0.06	0.08	2.008	2.742
	1.072	-	0.00	-1	-1	0.05	0.15		
	1.507	-	0.06	-1	+1	0.12	0.05		
	3.329	-	0.02	+1	-1	0.11	0.13		
^{160}Yb	0	3.085	0.00	+1	+1	0.06	0.06	3.438	3.06
	1.629	-	0.00	-1	-1	0.05	0.13		
	1.858	-	0.02	-1	+1	0.11	0.05		
	3.893	-	0.02	+1	-1	0.10	0.12		

TABLE III: Excitation energies, correlation energies and dynamical deformations of the lowest four states obtained in 2-dim GCM. $\Delta_{16/25}$ denotes the difference in energies between calculations performed with 16 and 25 mean-field states. π and π_{xy} denote the parity and P_{xy} quantum numbers, respectively. In the last two columns the two-quasiparticle excitation energies (neutron and proton) of the spherical configuration are given.

SLy4	a	b
⁹⁸ Zr	0.78	1.05
¹¹⁰ Zr	0.67	0.72
¹⁵² Gd	0.83	0.90
¹⁵⁴ Gd	0.97	0.91
¹⁵⁶ Gd	1.15	0.89
¹⁶⁰ Yb	1.04	1.12

TABLE IV: Ratios of the B(E3) values obtained for the transitions between the four lowest GCM states. In the column denoted by a , the ratio is taken between $|\Phi_{--}\rangle \rightarrow |\Phi_{++}\rangle$, and $|\Phi_{-+}\rangle \rightarrow |\Phi_{++}\rangle$, and in b for: $|\Phi_{+-}\rangle \rightarrow |\Phi_{--}\rangle$ and $|\Phi_{+-}\rangle \rightarrow |\Phi_{-+}\rangle$.

